An increased CD25-positive intestinal regulatory T lymphocyte population is dependent upon Cox-2 activity in the $Apc^{min/+}$ model

O. O. Faluyi [ID],*[†] P. Fitch[†] and
S. E. M. Howie[†]

*Edinburgh Cancer Centre, Western General
Hospital, and [†]MRC Centre for Inflammation
Research, University of Edinburgh, The Queen's
Medical Research Institute, Edinburgh, UK

Postal address: Department of Medical
Oncology, Clatterbridge Cancer Centre,
Bebington, Wirral CH63 4JY, UK.

Summary

Only mismatch repair (MMR)-deficient colorectal cancer (CRC) appears to respond well to programmed death (PD)-1 inhibition at the present time. Emerging evidence suggests a role for micro-environmental factors such as $CD25^+$ cells modulating response to PD-1 inhibition. In the $Apc^{Min/+}$ model of familial adenomatous polyposis (MMR-proficient CRC), increased Cyclooxygenase-2 (Cox-2) expression by cells which include alternatively activated mononuclear phagocytes promotes intestinal tumorigenesis by mechanisms which may include immune suppression. To gain insight into this, we compared regulatory T cell (T_{reg}) populations between $Apc^{Min/+}$ and wild-type mice prior to and after the phase of increased intestinal Cox-2-dependent prostaglandin E_2 (PGE_2) production. There was no difference in systemic T_{reg} function or numbers between $Apc^{Min/+}$ and wild-type mice. However, increased numbers of small intestinal $CD25^+$ T_{regs} were observed with increased Cox-2 activity in the absence of any difference in the expression of $Tgf-\beta$ or $Tslp$ between $Apc^{Min/+}$ and wild-type mice. Cox-2 inhibitor therapy (Celecoxib) reversed the increase in $Apc^{Min/+}$ intestinal $CD25^+$ T_{reg} numbers, without decreasing numbers of $CD25^+$ systemic T_{regs}. Forkhead box protein 3 ($FoxP3^+$) and $Cox-2^+$ cells were co-localized to the interstitium of adenomas of $Apc^{min/+}$ mice. These results suggest selective dependence of an 'activated T_{reg}' phenotype on paracrine Cox-2 activity in $Apc^{Min/+}$ small intestine. For therapeutic potential, further studies are required to evaluate the relevance of these findings to human cancer as well as the functional significance of $CD25^+$ intestinal T_{regs} in cancer.

Keywords: Cox-2, intestine, regulatory T cell, TGF-β, tumorigenesis

Introduction

Systemic therapy has led to some improvement in survival for patients with advanced colorectal cancer (CRC) during the past few decades; however, it remains a major cause of cancer-related mortality in the western world [1]. Therapeutic reversal of programmed death 1 (PD-1)/programmed death ligand 1 (PD-L1) pathway-mediated cancer immune suppression has emerged recently as a potent therapeutic target in some forms of cancer, but has not been effective for the majority of metastatic CRC except for those with mismatch repair (MMR) deficiency [2]. This observation is surprising, as there are relatively similar levels of PD-L1 expression between MMR-proficient and -deficient cancers [3]. A lower mutational burden resulting in reduced neo-epitopes in MMR-proficient cancer has been hypothesized as

one factor explaining reduced responsiveness to antagonism of immunosuppression [2]. However, emerging evidence suggests that tumour immune alterations beyond PD-L1 expression may also modulate responsiveness to PDL-1/PD-1 pathway antagonism. A recent study reported significantly enhanced response to PD-1 inhibition following depletion of $CD25^+$ cells [4].

Cyclooxygenase-2 (Cox-2) over-expression is associated ubiquitously with intestinal adenomas of familial adenomatous polyposis (FAP) [5] and more than 70% of sporadic colorectal adenomas [6]. However, up to half of MMR-deficient CRC may not over-express Cox-2 [7], while lower levels of Cox-2 over-expression have been reported for the others [8]. In contrast to most other mammalian tissues where Cox-2 is an inducible gene, Cox-2 is

expressed constitutively by intestinal lamina propria mono-nuclear cells (LPMNCs), where it has been shown to play a role in the establishment of dietary immune tolerance [9]. The observation that prostaglandin E$_2$ (PGE$_2$) can induce regulatory phenotype in CD4$^+$ T lymphocytes (T$_{regs}$) [10] has suggested a mechanism for Cox-2 in immune suppression. We have shown previously that intestinal LPMNC Cox-2-dependent PGE$_2$ production increases in C57BL/6 mice after the age of weaning ($\sim$ 4 weeks of age), with further up-regulation of intestinal LPMNC Cox-2-dependent PGE$_2$ production in the $Apc^{Min/+}$ model of FAP during the phase of appearance of macroscopic adenomas [11]. Our study and others [11–13] have suggested that macrophages, fibroblasts and vascular endothelial cells are the predominant source of intestinal Cox-2 expression in Apc mutant mice. Furthermore, CD4-T$_{reg}$ adoptive transfer led paradoxically to intestinal adenoma regression and reduced Cox-2 expression in the $Apc^{Min/+}$ model [14]. Conversely, adoptive transfer of naive CD4$^+$ T lymphocytes had the opposite effect of promoting intestinal tumorigenesis in the $Apc^{Min/+}$ mouse in association with inflammatory mononuclear infiltrates [15]. This has suggested a potential interaction between T$_{regs}$ and mononuclear phagocytes in the intestinal micro-environment to modulate intestinal tumorigenesis.

To yield insight into the role of Cox-2 expression in intestinal immune changes, we compared intestinal regulatory CD4-lymphocyte populations between $Apc^{Min/+}$, Cox-2 inhibitor-treated $Apc^{Min/+}$ and wild-type mice. We also studied T$_{reg}$ association with Cox-2 expressing cells.

Materials and methods

Animals

All animal work was carried out with appropriate UK Home Office and local ethical committee approval. $Apc^{Min/+}$ and $Apc^{+/+}$ (wild-type) mice on the C57BL/6 background obtained from the Jackson Laboratory (Bar Harbor, ME, USA) were bred according to UK Home Office guidelines under specific pathogen-free conditions at the University of Edinburgh and had free access to water and a standard RM1 diet (DBM, Livingston, UK). Some $Apc^{Min/+}$ mice were fed an RM1^{TM} diet containing 300 parts per million (p.p.m.) of Celecoxib (Pfizer, Madison, NJ, USA) from weaning (approximately 4 weeks of age) until analysis.

Adenoma counts and intestinal epithelial or LPMNC isolation

Mice were killed by a schedule 1 method (cervical dislocation). Intestinal adenomas were counted macroscopically by O.O.F., blinded to mouse diet. After removing visible Peyer's patches, intestinal LPMNCs were isolated as described previously [9]. LPMNC viability was assessed by trypan blue exclusion. Viability generally ranged between 75 and 85%. Intestinal epithelial cells obtained during the ethylenediamine tetraacetic acid (EDTA) (Invitrogen, Paisley, UK) incubation phase of LPMNC isolation were lysed in TRIZOL^{TM} (Invitrogen) and stored at $-20°C$ for real-time polymerase chain reaction (PCR) analysis. LPMNCs obtained after enzymatic digestion of residual intestinal tissue were washed in phosphate-buffered saline (PBS) containing 5% fetal calf serum (FCS) (Sigma, Poole, UK) and used for flow cytometric analysis.

Tissue processing

Mice at $\sim$ 4 (range = 4–5) or 15 (range = 14–16) weeks of age were culled and small intestine dissected out from the pylorus to the ileo–caecal junction. Intestinal lumina were flushed out with PBS until no luminal content was evident. The intestinal tissue was then opened longitudinally, segments fixed in methacarn (60% methanol, 30% chloroform and 10% glacial acetic acid) were dehydrated in ethanol and embedded in wax; 5-μm sections were obtained from wax-embedded tissue.

Immunohistochemistry (IHC)

Forkhead box protein 3 (FoxP3). Anti-FoxP3 antibody (e-Bioscience, Hatfield, UK) and anti-CD3 antibody (Dako, Ely, UK) IHC staining was carried out on methacarn fixed tissue as described [14]. Antigen retrieval was by means of Borg decloaker (Biocare Medical, Pacheco, CA, USA). FoxP3 staining was visualized with diaminobenzidine (DAB) from Dako and CD3 with Vector blue (Vector Labs, Peterborough, UK). The number of positive cells for either of these markers was determined by counting from 10 alternate villi in distal small intestine. Anti-transforming growth factor (TGF)-β antibody (R&D Systems, Abingdon, UK) IHC was carried out as described previously and developed with DAB [16]. Single-stained sections were counterstained with Mayer's haematoxylin.

Dual immunohistochemistry

Cox-2. Methacarn-fixed intestinal sections were stained with 10 μg/ml of affinity-purified rabbit anti-mouse Cox-2 antibody (160126; Cayman Chemicals, Ann Arbor, MI, USA) overnight at 4°C. Controls included Cox-2 antibody mixed with $\times$10 its concentration of its competing peptide (360106; Cayman Chemicals). An anti-rabbit secondary antibody was used, with development of staining with DAB [17]. Sections were then washed in PBS and underwent FoxP3 immunohistochemistry as described above, except that staining was developed with alkaline phosphatase rather than DAB.

Flow cytometry

Cell surface markers. Inguinal lymph node (ILN) ($\sim$ 5 $\times$ 10^5) or intestinal mononuclear cells were

resuspended in fluorescence activated cell sorter (FACS) buffer (2% FCS). After an Fc block (BD Biosciences, Oxford, UK) for 30 min, cells were labelled with CD4-FITC (2 × 5 µg/ml) and/or CD25-phycoerythrin (PE) (1 × 25 µg/ml) or concentration-matched isotype control (all e-Biosciences) for 30 min and then washed in FACS buffer. Intracellular staining was then carried out.

Intracellular staining. ILN ($\sim 5 \times 10^{5)}$ or intestinal mononuclear cells were resuspended in FACS buffer (2% FCS). After Fc blocking as above, cells were labelled with surface markers or concentration-matched isotype control (e-Biosciences) for 30 min and washed in FACS buffer. Cells were then fixed and permeabilized using the T_{reg} flow cytometry kit (e-Biosciences), according to the manufacturer's instructions. Subsequently, cells were stained with FoxP3-allophycocyanin (APC) (1 × 25 µg/ml) or concentration-matched isotype control (e-Biosciences) with or without an antibody to Helios (Helios-Alexa Fluor 647, from BioLegend, San Diego, CA, USA) or concentration-matched isotype control, as per the manufacturer's instructions. Cells were then washed and resuspended in FACS buffer.

Flow cytometry data acquisition was carried out on a FACSCalibur (BD Biosciences) using Cell Quest™ software. Cells within a viable lymphocyte gate were analysed with FloJo™ software (Tree Star, Inc., Ashland, OR, USA).

Regulatory T lymphocyte isolation and functional assays. ILN and spleens were obtained by dissection and passed through 40-µm filters (BD Biosciences, Oxford, UK) into 5% FCS in PBS. Splenic and ILN mononuclear cells were washed in 5% FCS and $CD4^+CD25^+$ (regulatory) and $CD4^+CD25^-$ (helper-inducer) populations were isolated using a T_{reg} isolation kit (Miltenyi Biotec, Woking, UK), according to the manufacturer's instructions; 5 × 10^4 $CD4^+$ $CD25^-$ cells/well in 96-well tissue culture plates were stimulated with CD3/CD28 microbeads (Invitrogen), according to the manufacturer's instructions, and then cultured alone or with an equal number of $CD4^+CD25^+$ cells. Unstimulated $CD4^+CD25^-$ cells served as controls. Cultures were pulsed with 1 µCi [^{3}H]-thymidine (Perkin Elmer, Cambridge, UK) per well after 72 h and then incubated for a further 24 h, after which the plates were frozen at −20°C until harvested and incorporated [^{3}H]-thymidine counted in a β-scintillation counter.

Real-time PCR analysis. RNA was isolated from cells lysed in TRIZOL as advised by the manufacturer. Subsequently, cDNA was generated using a reverse transcription kit (Invitrogen). Genomic contamination was excluded using intron spanning primers to *Cox-1* (forward: CAC AGT GCG GTC CAA CCT TAT, reverse: GAT GTA GTC ATG CGC TGA GTT GT) and looking for genomic-DNA sized PCR products on 2% agarose gels. Otherwise, real-time PCR was carried out with the following primers: *Hprt* (forward: TGA AAG ACT TGC TCG AGA TGT CA, reverse-

CAC ACA GAG GGC CAC AAT GT); *Tgf-β1* (forward: GCA GTG GCT GAA CCA AGG A, reverse: AGC AGT GAG CGC TGA ATC G); and *Tslp* (forward: CCC TGG CTG CCC TTC ACT, reverse CAT TGA GGG CTT CTC TTG TTC TC). All PCR primers were obtained from Invitrogen. PCR was then carried out on an Applied Biosystems 7700 machine using SYBR-green™ dye for fluorescence detection. PCR conditions were an annealing temperature of 60°C for 30s, then amplification for 60 s at 72°C for 40 cycles followed by 72°C for 10 min. The level of expression of *Tgf-β1* (*Tgf-β*) or *Tslp* was normalized to the housekeeping gene *Hprt*.

Statistics. Group data are summarized and presented as the mean value ± standard error of the mean. Data were analysed by Mann–Whitney using Prism™ software. Differences were considered statistically significant at a *P*-value of < 0·05.

Results

Increased numbers of FoxP3$^+$ small intestinal T lymphocytes in *Apc*$^{Min/+}$ compared with wild-type mice

We compared T_{reg} (FoxP3-expressing cell) numbers between *Apc*$^{Min/+}$ (n=3) and wild-type ($n = 3$) mouse small intestine at 15 weeks of age. CD3 (as a pan-T lymphocyte marker) was used to control for the total number of T lymphocytes. Double IHC showed that all FoxP3$^+$ cells were also CD3$^+$ (Fig. 1b). FoxP3$^+$ cells were localized to the lamina propria (LP) of intestinal villi in *Apc*$^{Min/+}$ and wild-type mice (Fig. 1b). However, FoxP3$^+$ cells were also localized to the interstitium of intestinal adenomas in *Apc*$^{Min/+}$ mice, particularly in a subepithelial location (shown later in Fig. 3). The number of FoxP3$^+$ cells per villus in *Apc*$^{Min/+}$ mouse small intestine was more than double the number observed in wild-type littermates, despite no significant difference in the number of CD3$^+$ cells (Fig. 1d,e). Consequently, we demonstrate increased numbers of FoxP3$^+$ T lymphocytes in *Apc*$^{Min/+}$ mouse intestine with established adenomas.

Increased proportion of *Apc*$^{Min/+}$ mouse FoxP3$^+$ small intestinal lymphocytes with age

We then compared LP and ILN populations between *Apc*$^{Min/+}$ and wild-type mice at 4 and 15 weeks of age (Fig. 2) in order to determine if the increased FoxP3$^+$ lymphocyte population of *Apc*$^{Min/+}$ small intestine occurred with age (during the phase of increased Cox-2 dependent PGE$_2$ production) and, furthermore, if populations in the intestine reflected those in unconnected lymphoid tissue.

The FoxP3$^+$ proportion of LP or ILN lymphocytes was similar between *Apc*$^{Min/+}$ and wild-type mice at 4 weeks of age (Fig. 2d). However, there was a significantly increased

Fig. 1. Increased numbers of forkhead box protein 3 (FoxP3)$^+$ cells in the intestinal villi of $Apc^{Min/+}$ mice at 15 weeks of age. (a–e) Immunohistochemistry, black bars = 30 μm. (a) Histologically normal distal small intestine from a wild-type (wt) mouse, no primary antibody control. (b) Histologically normal distal small intestine from $Apc^{Min/+}$ mouse showing nuclear FoxP3$^+$ (brown) and membrane CD3$^+$ (blue) staining in the lamina propria as well as an intra-epithelial location. (c) Spleen from an $Apc^{Min/+}$ mouse showing peri-arteriolar FoxP3$^+$ and CD3$^+$ cells in the marginal zone. (d) Numbers of FoxP3$^+$ cells per villus are significantly increased in $Apc^{Min/+}$ mice compared to wt mice (Mann–Whitney U-test). (e) Number of CD3$^+$ cells per villus are not significantly different in $ApcMin/+$ mice compared to wt mice.
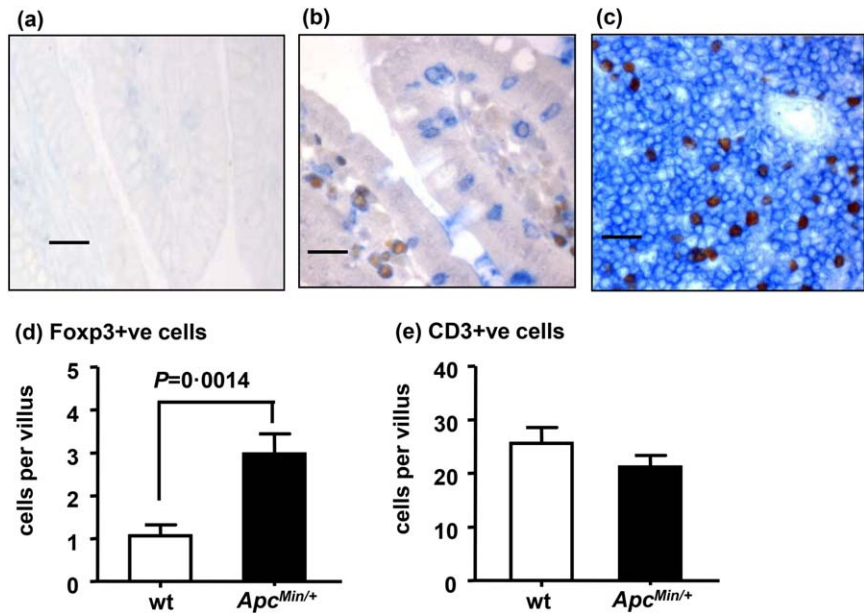
proportion of FoxP3$^+$ LP lymphocytes in $Apc^{Min/+}$ mice ($P = 0.012$) but not wild-type mice ($P = 0.19$) between 4 and 15 weeks of age (Fig. 2e). In particular, a significantly increased proportion of FoxP3$^+$ LP lymphocytes was observed in $Apc^{Min/+}$ compared with wild-type mice at 15 weeks of age ($P = 0.019$), with no significant difference in the proportion of FoxP3$^+$ ILN lymphocytes (Fig. 2e).

Alterations in the intestinal CD8 T lymphocyte population of the $Apc^{Min/+}$ mouse during tumorigenesis have been reported [18]. We therefore determined the CD4$^+$ population of regulatory T lymphocytes in $Apc^{Min/+}$ mice. CD4 and FoxP3 expression by LP or ILN lymphocytes of $Apc^{Min/+}$ and wild-type mice were analysed (Fig. 2f,g). The CD4$^+$ proportion of FoxP3$^+$ LP or ILN lymphocytes (range = 81–91%) was similar between $Apc^{Min/+}$ and wild-type mice. Consequently, during the phase of increased Cox-2-dependent PGE$_2$ production, we demonstrated an increased (predominantly CD4$^+$) regulatory intestinal lymphocyte population in $Apc^{Min/+}$ mice. Changes of a similar nature were not observed in inguinal lymph nodes.

An increased CD25$^+$ regulatory T lymphocyte population during tumorigenesis in $Apc^{Min/+}$ mouse intestine

IL-2 receptor-alpha (CD25) is a low-affinity IL-2 receptor expressed by T$_{regs}$ and activated lymphocytes [19]. We therefore analysed FoxP3 and CD25 expression by LP CD4 lymphocytes of $Apc^{Min/+}$ and wild-type mice to determine the phenotype of the increased T$_{reg}$ population occurring during the phase of increased Cox-2 expression (Fig. 2h,i).

As observed previously, a significantly increased CD4$^+$FoxP3$^+$ proportion of LP lymphocytes was observed in 15-week-old $Apc^{Min/+}$ compared with wild-type mice

(Fig. 2i). Even though the CD25$^+$ proportion of CD4$^+$FoxP3$^+$ lymphocytes was reduced in wild-type intestine compared to ILN (Fig. 2h,i), the CD25$^+$ proportion of CD4$^+$FoxP3$^+$ LP lymphocytes was higher in 15-week-old $Apc^{Min/+}$ than wild-type mice ($P = 0.002$) (Fig. 2i).

Cox-2-inhibitor therapy inhibits small intestinal tumorigenesis and prevents the increase in CD4$^+$FoxP3$^+$CD25$^+$ lymphocytes in the $Apc^{Min/+}$ mouse

We determined initially if Cox-2 inhibitor therapy (with Celecoxib 300 parts ppm) prevented intestinal tumorigenesis in $Apc^{Min/+}$ mice, as described previously [16]. Figure 3a shows that Celecoxib treatment led to an 85% reduction in intestinal adenoma numbers in $Apc^{Min/+}$ mice.

We then determined the effect of Cox-2 inhibition on the T$_{reg}$ population of 15-week-old $Apc^{Min/+}$ mice. Celecoxib therapy had no significant effect on the CD25$^+$ proportion of the CD4$^+$FoxP3$^+$ ILN lymphocytes (Fig. 3b). However, the increased CD25$^+$ proportion of CD4$^+$FoxP3$^+$ LP lymphocytes of $Apc^{Min/+}$ compared with wild-type mice was reduced by Celecoxib treatment (Fig. 3c). This suggested that the increased CD25$^+$ intestinal T$_{reg}$ population of $Apc^{Min/+}$ mice was dependent upon Cox-2 activity. Notably, there was no significant difference in the proportion of CD4$^+$FoxP3$^+$ intestinal lymphocytes between Cox-2 inhibitor-treated $Apc^{Min/+}$ mice ($24.56 \pm 0.59\%$; $n = 4$) and those fed a control diet ($24.12 \pm 2.18\%$; $n = 8$) ($P = 0.933$). This suggested that even though Cox-2 inhibition decreased the CD25$^+$ intestinal T$_{reg}$ population, it did not decrease the total intestinal T$_{reg}$ population.
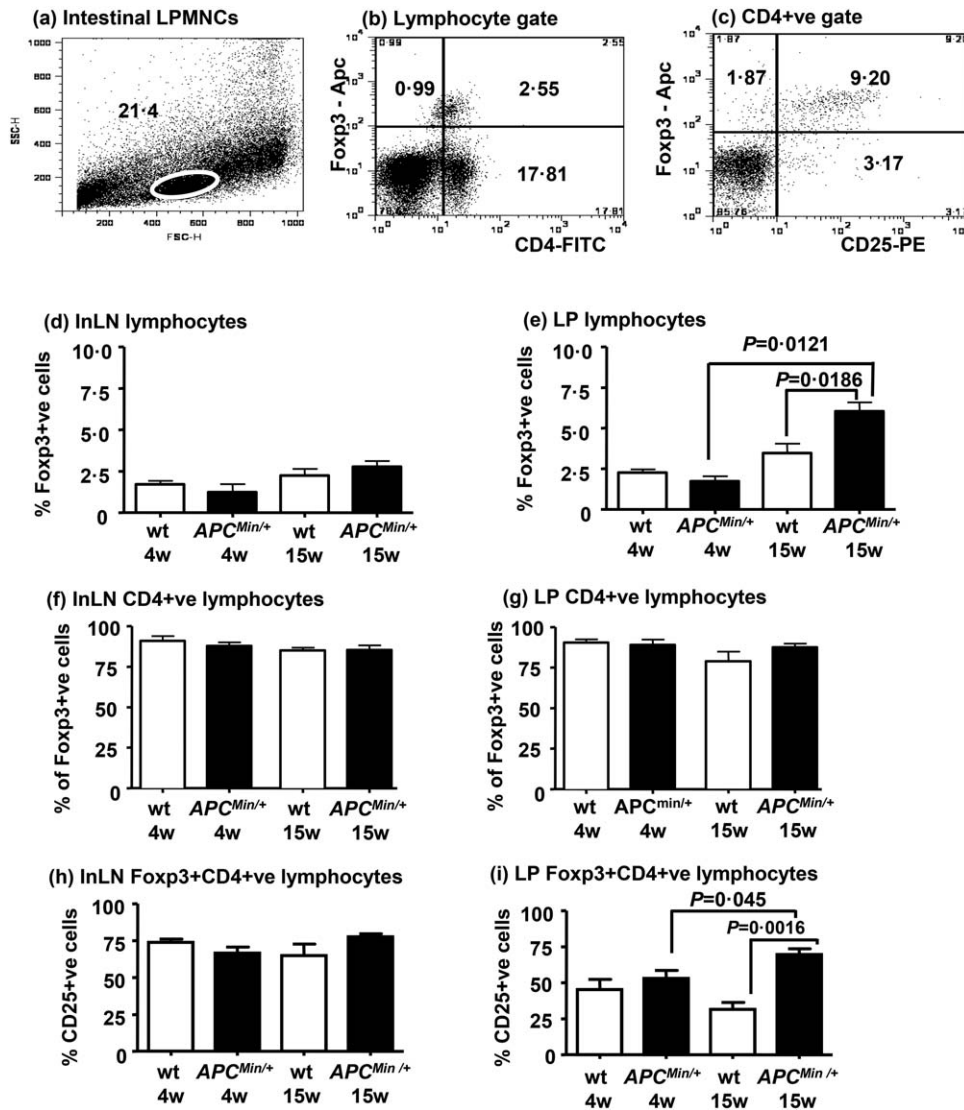
Fig. 2. Analysis of FoxP3$^+$ lymphocyte populations in inguinal lymph nodes and intestinal lamina propria (LP) of wild-type (wt) and $Apc^{Min/+}$ mice. (a–c) Representative flow cytometry plots of intestinal lamina propria mononuclear cells (LPMNCs) showing (a) the viable lymphocyte gate on a forward- *versus* side-scatter plot; (b) the % of FoxP3$^+$ and CD4$^+$ cells within the viable lymphocyte gate and (c) the % of FoxP3$^+$ and CD25$^+$ cells within lymphocytes gated for CD4 expression. (d) There are no significant differences between the % of forkhead box protein 3 (FoxP3)$^+$ lymphocytes in inguinal lymph nodes (InLN) of wt (open boxes) or $Apc^{Min/+}$ (black boxes) mice at 4 or 15 weeks of age. (e) There is no significant difference between the % of FoxP3$^+$ lymphocytes in the LP of mice at 4 weeks of age. In contrast, there is an increase in the % of FoxP3$^+$ lymphocytes in the LP of $Apc^{Min/+}$ mice at 15 weeks compared to wt mice of the same age and to 4-week-old $Apc^{Min/+}$ mice. (f,g) There are no significant differences in the % of FoxP3$^+$ cells that are also CD4$^+$ in InLN (f) or LP (g) between wt and $Apc^{Min/+}$ mice at 4 or 15 weeks of age. (h) The proportion of FoxP3$^+$CD4$^+$ cells that are CD25$^+$ does not change with age in inguinal lymph nodes and is similar between wt and $Apc^{Min/+}$ mice. (i) Compared to lymph node lymphocytes, there is a decreased proportion of CD25$^+$FoxP3$^+$CD4$^+$ cells in lamina propria lymphocytes. There is no difference in this subset between wt and $Apc^{Min/+}$ mice at 4 weeks of age, whereas it is increased significantly in $Apc^{Min/+}$ mice at 15 weeks of age compared to wt mice of the same age and to $Apc^{Min/+}$ mice at 4 weeks of age. Data are shown as mean ± standard error of the mean (s.e.m.) of three to six mice per group. Statistical comparisons by Mann–Whitney *U*-test.

FoxP3 and Cox-2 expressing cells are co-localized to the interstitium of $Apc^{Min/+}$ small intestinal adenomas

The distribution of FoxP3$^+$ cells in this study (Figs 1 and 3) was similar to the distribution of Cox-2$^+$ cells in our previous study [11] and those of others [12]. Therefore, to substantiate the possibility of paracrine interaction between T$_{regs}$ and *Cox-2* expressing mononuclear phagocytes, we carried out co-immunohistochemistry for FoxP3 and Cox-2 expression on intestinal adenomas of $Apc^{Min/+}$ mice. FoxP3 and Cox-2 expressing cells were co-localized to the interstitium of intestinal adenomas (Fig. 3g).
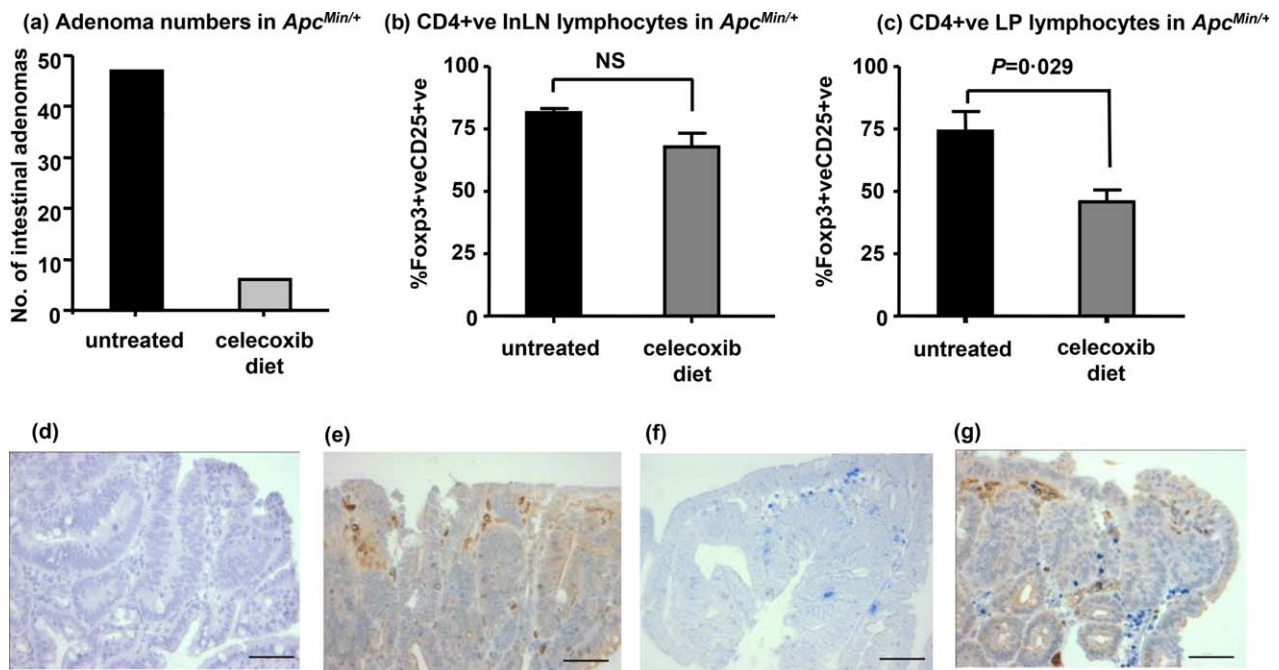
Fig. 3. Celecoxib treatment reduces the proportion of CD4$^+$forkhead box protein 3 (FoxP3)$^+$CD25$^+$ lamina propria but not inguinal lymph node lymphocytes of $Apc^{Min/+}$ mice at 15 weeks of age. (a) Celecoxib reduces the numbers of $Apc^{Min/+}$ mouse intestinal adenomas. (b) Celecoxib has no significant effect on the proportion of $Apc^{Min/+}$ mouse inguinal lymph nodes (InLN) cells with a conventional regulatory T cell (T$_{reg}$) phenotype. (c) Decreased proportion of CD4$^+$FoxP3$^+$CD25$^+$ cells in intestinal lamina propria (LP) lymphocytes of $Apc^{Min/+}$ mice treated with celecoxib. (d–g) Co-immunohistochemistry for Cox-2 and FoxP3 protein localization was carried out on $Apc^{Min/+}$ mouse small intestinal adenomas. (d) Adenomatous small intestine from an $Apc^{Min/+}$ mouse, showing no staining with Cox-2 pre-incubated with the competing peptide. (e) Adenomatous small intestine from an $Apc^{Min/+}$ mouse, showing staining with Cox-2 (brown cells). (f) Adenomatous small intestine from an $Apc^{Min/+}$ mouse showing staining with FoxP3 (blue cells). (g) Adenomatous small intestine from an $Apc^{Min/+}$ mouse adenoma co-localizing Cox-2 (brown cells) and FoxP3 (blue cells) (scale bar = 50 μm).

No impairment of CD4-regulatory T lymphocyte function in $Apc^{Min/+}$ mice

Lymphocytic developmental defects have been described in mice with constitutive β-catenin signalling [20], such as occurs in Apc mutant mice. We therefore tested for possible defective function of $Apc^{Min/+}$ mouse CD4$^+$ T$_{regs}$ accounting for their increased numbers in the immune active intestinal micro-environment. CD4$^+$CD25$^-$ (helper) and CD4$^+$CD25$^+$ (regulatory) T lymphocytes were isolated from splenic and ILN lymphocytes of $Apc^{Min/+}$ mice ($n = 3$) and wild-type mice ($n = 3$) at 15 weeks of age. The percentage suppression of CD3CD28-induced T lymphocyte proliferation by regulatory T lymphocytes was 62·8 ± 16·1% for $Apc^{Min/+}$ compared to 59·9 ± 9·1% for wild-type mice. Therefore, we did not observe any impairment of $Apc^{Min/+}$ mouse peripheral T$_{reg}$ functional ability.

Helios expression by intestinal regulatory lymphocytes of $Apc^{Min/+}$ mice

Helios expression has been reported to stabilize T$_{reg}$ function [21]. We further characterized the increased intestinal T$_{regs}$ occurring after the phase of increased Cox-2-dependent PGE$_2$ production in $Apc^{Min/+}$ mice (Fig. 4).

We compared Helios expression by LP T$_{regs}$ of 15-week-old $Apc^{Min/+}$ and wild-type mice (Fig. 4). Among CD4$^+$FoxP3$^+$ LP lymphocytes, a significantly increased Helios$^+$ population was observed in $Apc^{Min/+}$ compared with wild-type mice ($P = 0·029$) (Fig. 4e). Furthermore, among CD4$^+$CD25$^+$ LP lymphocytes, increased Helios expression in $Apc^{Min/+}$ compared with wild-type mice ($P = 0·029$) was observed (Fig. 4f). This suggested that induced T$_{regs}$ during the phase of Cox-2 dependent PGE$_2$ production were predominantly CD25$^+$ and Helios$^+$ in $Apc^{Min/+}$ mice. In contrast, no significant differences were observed in the Helios$^+$ lymphocyte populations between ILN lymphocytes of $Apc^{Min/+}$ and wild-type mice (data not shown).

$Tslp$ and Tgf-β expression by small intestinal epithelial cells of $Apc^{Min/+}$ and wild-type mice at different ages

We then compared known molecular signals to T$_{reg}$ generation between $Apc^{Min/+}$ and wild-type mice. We compared small intestinal epithelial Tgf-β [22] and $Tslp$ [23] mRNA expression prior to and after the period of increased Cox-2 dependent PGE$_2$ production. Increased Tgf-β mRNA
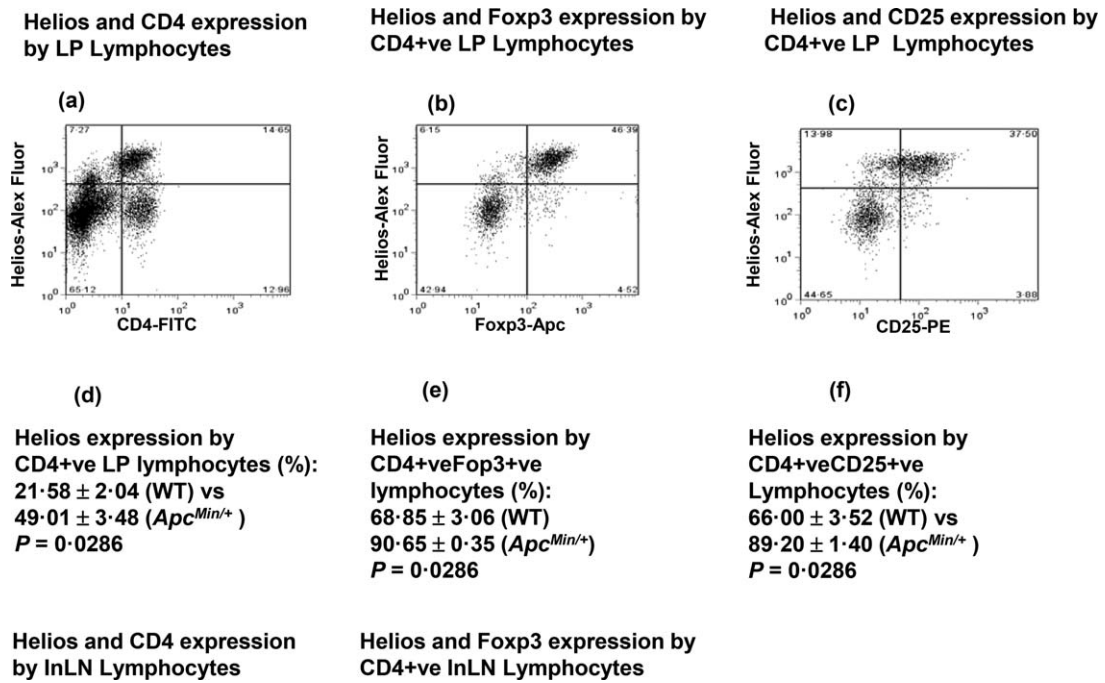
Helios and CD4 expression by LP Lymphocytes

(a)

Helios and Foxp3 expression by CD4+ve LP Lymphocytes

(b)

Helios and CD25 expression by CD4+ve LP Lymphocytes

(c)

(d)

Helios expression by CD4+ve LP lymphocytes (%):
21·58 ± 2·04 (WT) vs
49·01 ± 3·48 ($Apc^{Min/+}$)
P = 0·0286

(e)

Helios expression by CD4+veFop3+ve lymphocytes (%):
68·85 ± 3·06 (WT)
90·65 ± 0·35 ($Apc^{Min/+}$)
P = 0·0286

(f)

Helios expression by CD4+veCD25+ve Lymphocytes (%):
66·00 ± 3·52 (WT) vs
89·20 ± 1·40 ($Apc^{Min/+}$)
P = 0·0286

Helios and CD4 expression by InLN Lymphocytes

Helios and Foxp3 expression by CD4+ve InLN Lymphocytes

Fig. 4. Increased proportions of Helios^{+}forkhead box protein 3 (FoxP3)[+]CD25^{+} small intestinal regulatory T lymphocytes in $Apc^{Min/+}$ mice at 15 weeks of age. (a–c) Representative flow cytometry plots of intestinal lamina propria mononuclear cells (LPMNCs) showing: (a) The % of Helios and CD4^{+} cells within viable lymphocytes of an $Apc^{Min/+}$ mouse. (b) The % of Helios^{+} and FoxP3^{+} cells within viable lymphocytes of an $Apc^{Min/+}$ mouse gated for CD4 expression. (c) The % of Helios^{+} and CD25^{+} cells within viable lymphocytes of an $Apc^{Min/+}$ mouse gated for CD4 expression. (d) There is a significantly increased LP Helios^{+} CD4-lymphocyte population in $Apc^{Min/+}$ compared with wild-type mice. (e) There is a significantly increased LP Helios^{+}FoxP3^{+} CD4-lymphocyte population in $Apc^{Min/+}$ compared with wild-type mice. (f) There is a significantly increased LP Helios^{+}CD25^{+}CD4[-]lymphocyte population in $Apc^{Min/+}$ compared with wild-type mice.

expression was observed between 4 and 15 weeks of age in $Apc^{Min/+}$ and wild-type mice (Fig. 5a), but levels of *Tgf-β* mRNA expression were similar between $Apc^{Min/+}$ and wild-type mice at either age tested. In contrast, we observed a trend towards decreased small intestinal epithelial *Tslp* mRNA expression between 4 and 15 weeks of age in $Apc^{Min/+}$ and wild-type mice, but no difference in levels of

Tslp mRNA expression between $Apc^{Min/+}$ and wild-type mice at either age tested (Fig. 5b).

Discussion

To the best of our knowledge, this is the first description of an association between Cox-2 activity and T$_{reg}$
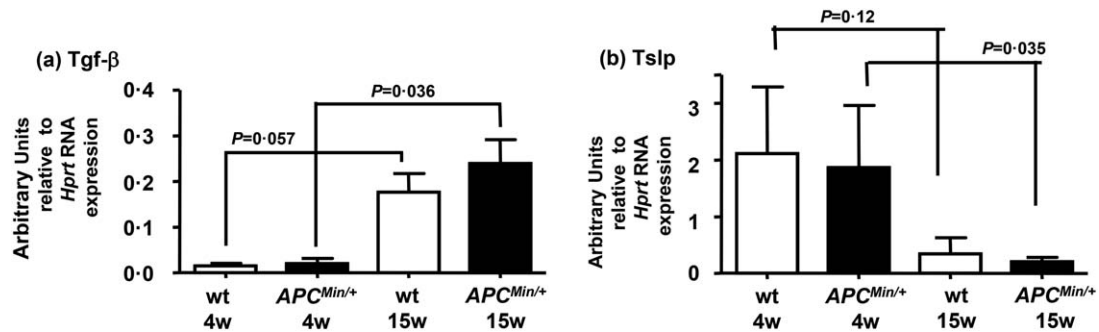

Fig. 5. *Tgf-β* and *Tslp* mRNA expression by small intestinal cells of wild-type (wt) and $Apc^{Min/+}$ mice. mRNA isolated from small intestinal epithelial cells of $Apc^{Min/+}$ (black boxes) and wt (open boxes) mice was analysed by real-time polymerase chain reaction (PCR) analysis. The fold expression of *Tgf-β* (a) or *Tslp* (b) relative to *Hprt* for individual mice is expressed in arbitrary units [three to five mice per group, data reported as mean ± standard error of the mean (s.e.m.)]. There was no difference between wt and $Apc^{Min/+}$ mice at either 4 or 15 weeks of age for mRNA of either gene. There was a significant increase in *Tgf-β* expression in $Apc^{Min/+}$ and an almost significant increase in wt mice at 15 weeks of age compared to younger mice (Mann–Whitney *U*-test). *Tslp* expression was more variable in the younger age group; although the results did not achieve significance, there was a trend for higher *Tslp* expression in younger animals of both genotypes.

phenotypical variation during intestinal tumorigenesis in the $Apc^{Min/+}$ model. We show an increased predominantly CD4$^+$ $Apc^{Min/+}$ small intestinal T$_{reg}$ population with age during the phase of adenoma development. This is consistent with previous reports of increased T$_{regs}$ in the tumor micro-environment [24]. Similarly, we previously showed induction of human T$_{regs}$ *in vitro* by a small-cell lung cancer cell line [25]. Perhaps the most important finding was a Cox-2-dependent increased CD25$^+$ intestinal T$_{reg}$ population which is Helios$^+$. We also demonstrate co-localization of T$_{regs}$ and Cox-2 expressing mononuclear phagocytes. Taken together, these suggest that paracrine interaction between Cox-2 expressing mononuclear phagocytes and T$_{regs}$ in $Apc^{Min/+}$ mouse intestine modulate the T$_{reg}$ phenotype.

Determining the functional significance of phenotypical observations reported here, as well as the relationship between Cox-2 and PD-1/PDL-1 expression, were beyond the scope of this study. However, diphtheria-toxin-mediated FoxP3-expressing cell depletion in the $Apc^{Min/+}$ mouse has been reported to increase intestinal T lymphocyte infiltrates with a proinflammatory stroma as a consequence [26]. Nevertheless, the functional significance of the CD25$^+$FoxP3$^+$ subpopulation in the intestinal immune microenvironment is not known. The recent observation that antibody-mediated depletion of CD25$^+$ cells in a mouse model enhanced response to PD-1 antagonism suggests their potential *in-vivo* relevance. CD25-null mice (*IL-2Rα*-null) had reduced sensitivity to IL-2, which compromised T lymphocyte function associated with polyclonal expansion of T lymphocytes [27]. With respect to T$_{regs}$, it is known that IL-2R–STAT-5-mediated signalling generates activated STAT-5, which is essential for stabilization of FoxP3 expression by binding the conserved non-coding sequence 2 (*CNS2*) region of the FoxP3 promoter [28]. Additionally, the Ikaros transcription factor *Helios* is known to have STAT-5b as one of its principal targets in mice, stabilizing STAT-5-dependent IL-2 responsiveness [21]. The observation that constitutive STAT-5b activation increased intestinal adenoma size in the $Apc^{Min/+}$ mouse is consistent with a role for IL-2R-–STAT-5 T$_{reg}$ activation in promoting intestinal tumorigenesis [29]. It is noteworthy that constitutive STAT-5b activation abrogated proinflammatory cytokine secretion while modifying expression of cell surface molecules by T lymphocytes [29]. These, taken together, suggest that abrogation of an increased intestinal CD25$^+$ T$_{reg}$ population during tumorigenesis in $ApcMin/^+$ mice by Cox-2 inhibition could impair T$_{reg}$ function, thus countering tumour immunosuppression. Our observation that the CD25$^+$ T$_{reg}$ population of unconnected lymph nodes is not increased during tumorigenesis and unaffected by Cox-2 inhibition suggests selectivity of the LP T$_{reg}$ phenotypical modification as a potential therapeutic target, compared to non-specific ablation of the CD25$^+$ population.

With regard to underlying mechanisms, the observation of an increased proportion of CD25$^-$ LP T$_{regs}$ and increased intestinal epithelial *Tgf-β* expression with age in wild-type mice would be consistent with the generation of adaptive T$_{regs}$ by TGF-β activity in intestinal immune tolerance [30]. However, there was no increase in levels of *Tgf-β* expression in $Apc^{Min/+}$ compared with wild-type small intestine to explain the further increase in the number of CD25$^-$ T$_{regs}$ observed with the inhibition of Cox-2 activity. The observation that Cox-2 inhibition is known to suppress the growth of adenomas greater than 1 mm in size, but does not abrogate adenoma growth completely, may explain this [31]. Consequently, one explanation for increased CD25$^-$ T$_{regs}$ in $Apc^{Min/+}$ with Cox-2 inhibition could be increased TGF-β derived from an increased number of intestinal epithelial cells within adenomas, rather than increased levels of *Tgf-β* expression in $Apc^{Min/+}$ mice. However, an alternative tumour-specific signal to LP T$_{reg}$ generation during the process of tumorigenesis (which was not the purpose of this study) cannot be excluded. With reference to our observations, it has been proposed that, in different circumstances, TGF-β can generate T$_{regs}$ via diverse molecular pathways [dependent upon or independent of CD25 signalling] [32]. Furthermore, a previous study showed conversion of CD25$^-$ T$_{regs}$ to CD25$^+$ T$_{regs}$ by TGF-β to mediate immunosuppression in tumours [33]. Of possible relevance to this is the fact that TGF-β has been shown to induce alternative activation of mononuclear phagocytes [34]. Our study suggests that Cox-2 inhibition reverses paracrine effects of alternately activated macrophages to enhance CD25 expression in T$_{regs}$ of the $Apc^{Min/+}$ intestinal micro-environment.

With regard to determining the clinical relevance of observations reported here, it would be important to determine if the phenotypical T$_{reg}$ change observed with Cox-2 inhibition in $Apc^{Min/+}$ intestine applies to CRC tumours and/or metastases in humans. Furthermore, future studies will need to define the functional significance of loss of the T$_{reg}$ IL-2 receptor with Cox-2 inhibition in the $Apc^{Min/+}$ intestinal tumour micro-environment. These could help to determine if there is a role for Cox-2 inhibition in enhancing immunotherapy for CRC.

Acknowledgements

Disclosure

None declared.

References

1 Ferlay J, Steliarova-Foucher E, Lortet-Tieulent J *et al.* Cancer incidence and mortality patterns in Europe: estimates for 40 countries in 2012. Eur J Cancer 2013; **49**:1374–403.

2 Le DT, Uram JN, Wang H *et al.* PD-1 blockade in tumors with mismatch-repair deficiency. N Engl J Med 2015; **372**:2509–20.

3 Droeser RA, Hirt C, Viehl CT *et al.* Clinical impact of programmed cell death ligand 1 expression in colorectal cancer. Eur J Cancer 2013; **49**:2233–42.

4 Arce Vargas F, Furness AJS, Solomon I *et al.* Fc-optimized anti-CD25 depletes tumor-infiltrating regulatory T cells and synergizes with PD-1 blockade to eradicate established tumors. Immunity 2017; **46**:577–86.

5 Khan KN, Masferrer JL, Woerner BM, Soslow R, Koki AT. Enhanced cyclooxygenase-2 expression in sporadic and familial adenomatous polyposis of human colon. Scand J Gastroenterol 2001; **36**:865 –9.

6 Chapple KS, Cartwright EJ, Hawcroft G *et al.* Localization of cyclooxygenase-2 in human sporadic colorectal adenomas. Am J Pathol 2000; **156**:545 –53.

7 Castells A, Payá A, Alenda C *et al.* Cyclooxygenase 2 expression in colorectal cancer with DNA mismatch repair deficiency. Clin Cancer Res 2006; **12**:1686–92.

8 Sinicrope FA, Lemoine M, Xi L *et al.* Reduced expression of cyclooxygenase 2 proteins in hereditary nonpolyposis colorectal cancers relative to sporadic cancers. Gastroenterology 1999; **117**:350–8.

9 Newberry RD, Stenson WF, Lorenz RG. Cyclooxygenase-2-dependent arachidonic acid metabolites are essential modulators of the intestinal immune response to dietary antigen. Nat Med 1999; **5**:900–6.

10 Baratelli F, Lin Y, Zhu L *et al.* Prostaglandin E2 induces FOXP3 Gene expression and T-regulatory cell function in human CD4+ T cells. J Immunol 2005; **175**:1483–90.

11 Hull MA, Faluyi OO, Ko CWS *et al.* Regulation of stromal cell cyclooxygenase-2 in the ApcMin/+ mouse model of intestinal tumorigenesis. Carcinogenesis 2006; **27**:382–91.

12 Shattuck-Brandt RL, Varilek GW, Radhika A, Yang F, Washington MK, DuBois RN. Cyclooxygenase 2 expression is increased in the stroma of colon carcinomas from IL-10(–/–) mice. Gastroenterology 2000; **118**:337–45.

13 Sonoshita M, Takaku K, Oshima M, Sugihara K, Taketo MM. Cyclooxygenase-2 expression in fibroblasts and endothelial cells of intestinal polyps. Cancer Res 2002; **62**:6846–9.

14 Erdman SE, Sohn JJ, Rao VP *et al.* CD4+CD25+ regulatory lymphocytes induce regression of intestinal tumors in Apc^Min/+ mice. Cancer Res 2005; **65**:3998–4004.

15 Rao VP, Poutahidis T, Ge Z *et al.* Proinflammatory CD4+CD45RBhi lymphocytes promote mammary and intestinal carcinogenesis in Apc^Min/+ mice. Cancer Res 2006; **66**:57–61.

16 Swamy MV, Patlolla JM, Steele VE, Kopelovich L, Reddy BS, Rao CV. Chemoprevention of familial adenomatous polyposis by low doses of atorvastatin and celecoxib given individually and in combination to APCMin mice. Cancer Res 2006; **66**:7370–7.

17 Cook CH, Bickerstaff AA, Wang J *et al.* Spontaneous renal allograft acceptance associated with "regulatory" dendritic cells and IDO. J Immunol 2008; **180**:3103 – 12.

18 Tanner SM, Daft JG, Hill SA, Martin CA, Lorenz RG. Altered T-cell balance in lymphoid organs of a mouse model of colorectal cancer. J Histochem Cytochem 2016; **64**:753–67.

19 Malek TR, Castro I. Interleukin-2 receptor signaling: at the interface between tolerance and immunity. Immunity 2010; **33**:153–65.

20 Coletta PL, Müller AM, Jones EA *et al.* Lymphodepletion in the Apc^Min/+ mouse model of intestinal tumorigenesis. Blood 2004; **103**:1050–8.

21 Kim HJ, Barnitz RA, Kreslavsky T *et al.* Stable inhibitory activity of regulatory T cells requires the transcription factor Helios. Science 2015; **350**:334–9.

22 Buzoni-Gatel D, Debbabi H, Mennechet FJD *et al.* Murine ileitis after intracellular parasite infection is controlled by TGF-beta producing intraepithelial lymphocytes. Gastroenterology 2001; **120**:914–24.

23 Taylor BC, Zaph C, Troy AE *et al.* TSLP regulates intestinal immunity and inflammation in mouse models of helminth infection and colitis. J Exp Med 2009; **206**:655–67.

24 Valzasina B, Piconese S, Guiducci C, Colombo MP. Tumor-induced expansion of regulatory T cells by conversion of CD4+CD25– lymphocytes is thymus and proliferation independent. Cancer Res 2006; **66**:4488–95.

25 Wang W, Hodkinson P, McLaren F *et al.* Small cell lung cancer tumour cells induce regulatory T lymphocytes, and patient survival correlates negatively with FOXP3(+) cells in tumour infiltrate. Int J Cancer 2012; **131**:E928–37.

26 Akeus P, Langenes V, Kristensen J *et al.* Treg-cell depletion promotes chemokine production and accumulation of CXCR3(+) conventional T cells in intestinal tumors. Eur J Immunol **45**:1654–66.

27 Willerford DM, Chen J, Ferry JA, Davidson L, Ma A, Alt FW. Interleukin-2 receptor alpha chain regulates the size and content of the peripheral lymphoid compartment. Immunity 1995; **3**:521–30.

28 Josefowicz SZ, Lu LF, Rudensky AY. Regulatory T cells: mechanisms of differentiation and function. Annu Rev Immunol 2012; **30**:531–64.

29 Chinen T, Kannan AK, Levine AG *et al.* An essential role for the IL-2 receptor in Treg cell function. Nat Immunol 2016; **17**:1322–33.

30 Neurath MF, Fuss I, Kelsall BL, Presky DH, Waegell W, Strober W. Experimental granulomatous colitis in mice is abrogated by induction of TGF-beta-mediated oral tolerance. J Exp Med 1996; **183**:2605–16.

31 Seno H, Oshima M, Ishikawa TO *et al.* Cyclooxygenase-2 and prostaglandin E(2) receptor EP(2)-dependent angiogenesis in Apc(Delta716) mouse intestinal polyps. Cancer Res 2002; **62**:506–11.

32 Ogawa C, Tone Y, Tsuda M, Peter C, Waldmann H, Tone M. TGF-β-mediated Foxp3 gene expression is cooperatively regulated by Stat5, Creb, and AP-1 through CNS2. J Immunol 2014; **192**:475–83.

33 Liu VC, Wong LY, Jang T *et al*. Tumor evasion of the immune system by converting CD4+CD25- T cells into CD4+CD25+ T regulatory cells: role of tumor-derived TGF-beta. J Immunol 2007; **178**:2883–92.

34 Tiemessen MM, Jagger AL, Evans HG, van Herwijnen MJ, John S, Taams LS. CD4+CD25+Foxp3+ regulatory T cells induce alternative activation of human monocytes/macrophages. Proc Natl Acad Sci USA 2007; **104**:19446–51.